Separation Science and Technology
Publication details, including instructions for authors and subscription information:
http://www.informaworld.com/smpp/title~content=t713708471

Parameters Affecting Magnetic Field-Flow Fractionation of Metal Oxide Particles

T. C. Schunk[a]; J. Gorse[a]; M. F. Burke[a]
[a] CHEMISTRY DEPARTMENT, UNIVERSITY OF ARIZONA, TUCSON, ARIZONA

To cite this Article Schunk, T. C. , Gorse, J. and Burke, M. F.(1984) 'Parameters Affecting Magnetic Field-Flow Fractionation of Metal Oxide Particles', Separation Science and Technology, 19: 10, 653 — 666
To link to this Article: DOI: 10.1080/01496398408060667
URL: http://dx.doi.org/10.1080/01496398408060667

SEPARATION SCIENCE AND TECHNOLOGY, **19**(10), pp. 653-666, 1984

Parameters Affecting Magnetic Field-Flow Fractionation of Metal Oxide Particles

T. C. SCHUNK, J. GORSE, and M. F. BURKE

CHEMISTRY DEPARTMENT
UNIVERSITY OF ARIZONA
TUCSON, ARIZONA 85721

Abstract

Magnetic field-flow fractionation (FFF) is a new separation technique particularly suited to separations involving particulate materials of high magnetic permeability. In this technique a magnetic field, generated by an electromagnet, is used to induce retention of particles in the FFF flow stream. This paper discusses the theoretical basis for magnetic FFF in terms of the fundamental retention equation of FFF and the magnetic force equation. Experimental data are presented which characterizes the magnetic field and the retention process. The resolution of single particles from dimeric aggregates is demonstrated based upon their difference in volume.

INTRODUCTION

Field-flow fractionation (FFF) is a separation technique for liquid dispersions of small particles. As developed primarily by Giddings et al., FFF has been applied to a variety of materials with particle sizes in the range of 0.001 to 10 μm (*1*). The basis of separation in a FFF channel is the differential migration provided by the parabolic solvent velocity profile in an open channel. Retention is provided by the application of an external force field perpendicular to the carrier solvent flow stream, (Fig. 1). Depending upon the degree of interaction of the particle material with the field, the particles are induced to migrate toward one wall of the channel. An exponential concentration profile, somewhat like an atmosphere, is thus established at this wall by the balance of the downward induced velocity (U) and normal diffusion (D) of the particles in the solvent, Fig. 2. The average height of this concentration distribution, $l = D/U$, determines the rate of

0149-6395/84/1910-0653$3.50/0

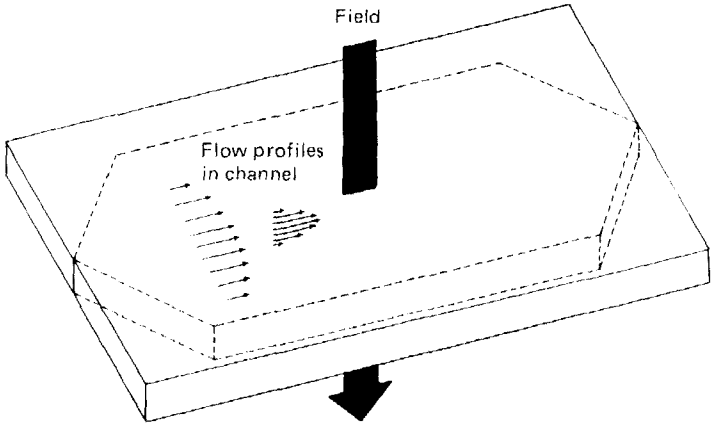

FIG. 1. Schematic diagram of field direction in a FFF channel.

migration of a specific group of particles by the mean velocity of the solvent at this height (*2*).

A number of different fields have been employed to achieve FFF separations by taking advantage of specific physicochemical properties of the particle materials (*3*). Giddings et al., have developed systems using gravitational (steric FFF) (*4*), inertial (sedimentation FFF) (*5*), thermal (thermal FFF) (*6*), electrical (electrical FFF) (*7*), and hydraulic (flow FFF) (*8*) fields.

As will be discussed in this paper, the use of a magnetic field in a FFF system is a new application particularly suited to the study of materials with high magnetic permeabilities [ferrimagnetic materials (*9*)], such as some metal oxide particles. To achieve retention with magnetic FFF an intense field which is uniform along the channel length is required and a high field gradient with height across the channel must be established. In order to meet these requirements in our experiments, a solenoid-type electromagnet was employed with the flow channel clamped directly on top of one pole face. By this means a magnetic field was generated, the intensity of which was easily varied by adjusting the current through the solenoid coil. The magnetic force is determined by both the intensity of the magnetic field and the magnitude of the field gradient (*9*). Retention of individual metal oxide particles is a function of the magnetic parmeabilities of the material and the solvent. Finally, as will be discussed, resolution of single particles from aggregates may be achieved because the force is a function of the volume of the particles.

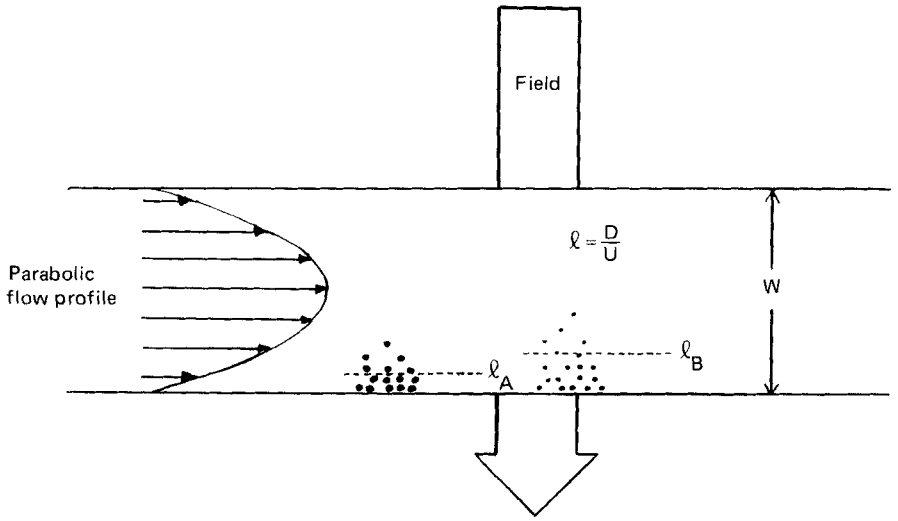

FIG. 2. Schematic diagram of flow profile and retained particle concentration distributions in a FFF channel.

THEORY

Field-Flow Fractionation Retention

The basic equations describing retention in a FFF system have been derived by Giddings et al. and verified with a variety of applied fields (*3*). Retention is expressed by the retention ratio $R = V^{\circ}/V_r$, the ratio of the system void volume to the component retention volume. Thus for retained species, R is always less than unity. Field flow conditions are established when the particle concentration distribution is in near equilibrium with the force field and diffusion. An exponential concentration distribution is obtained under these conditions, described by

$$c(x) = c_0 \exp(-x/l) \tag{1}$$

where c_0 is the concentration at the wall ($x = 0$) and l is the mean height of the particle distribution. By combining this equation with the laminar parabolic flow velocity equation, a general formula for retention in a FFF channel is obtained:

$$R = 6\lambda(\coth(1/2\lambda) - 2\lambda) \tag{2}$$

where λ is a dimensionless retention parameter equal to l/w. This equation is consistent with the classical equation describing the random thermal motion of particles in a force field (Langevin equation).

Giddings has shown that the dimensionless parameter λ may be expressed in terms of the balance of forces producing the particle concentration distribution. That is

$$\lambda = l/w = D/Uw = R'T/Fw \tag{3}$$

where w = channel height, D = particle diffusion coefficient, U = mean field-induced particle velocity, R' = gas constant, T = absolute temperature, and F = field-induced force.

Band Broadening

It is useful to consider the current understanding of FFF band broadening with respect to optimizing experimental conditions and separation speed. Since the quantitative theoretical predictions of FFF band broadening (*2, 10*), however, have not been as successfully supported by experiment as those for FFF retention, only trends can be indicated. The equation used is analogous to that for open tubular chromatography (*11*). The summation of variances describes plate height as a function of mean carrier solvent velocity $\langle v \rangle$,

$$H = \frac{2D}{R\langle v \rangle} + \frac{\chi w^2 \langle v \rangle}{D} + \sum H_i \tag{4}$$

The individual terms of this equation have been defined as:

Longitudinal diffusion: $2D/R\langle v \rangle$
Nonequilibrium mass transfer: $\chi w^2 \langle v \rangle / D$
Extraneous contributions: $\sum H_i$

where χ is a complex function of λ (*12*). It must be emphasized that this equation can be valid only for a solute which has reached its field-diffusion equilibrium state and is thus experiencing true field flow behavior. For this reason an initial stopped flow relaxation period is sometimes employed or the applied field is increased at the beginning of the separation to settle the particles close to the channel inlet (*5*). Either of these procedures allows field

flow behavior to occur over the largest possible fraction of the channel length.

The nonequilibrium mass transfer term has been shown to exhibit the primary role in determining channel performance (*12*). This term predicts an increase in channel efficiency or separation speed with increasing field strength and decreasing channel height (*2*).

Magnetic Force

As described in Eqs. (1) and (3), the distribution of particles in the FFF channel is determined by the tendency of particles to diffuse in the solvent and the downward velocity induced by the interaction of the particle material with the field. In magnetic FFF the magnitude of this downward velocity is determined by how strongly the metal oxide particles are attracted toward one pole of the magnet. This attraction may be expressed as a magnetic force F by the equation

$$F = \frac{(\mu_2 - \mu_1)}{8\pi} H \frac{dH}{dx} V \tag{5}$$

where μ_1 and μ_2 are the magnetic permeabilities of the solvent and the particle material, respectively, H is the magnetic field intensity, dH/dx is the magnetic field gradient, and V is the particle volume (*13*).

Equations (2) and (3) state that retention increases as the field-induced force increases, thus Eq. (5) predicts the changes in particle and field characteristics which would increase retention. Particle materials of high magnetic permeability and larger particles would show greater retention. In addition, maximizing the difference between the magnetic permeability of the sample and solvent should improve retention. However, since all common carrier solvents used in FFF are only weakly diamagnetic, this effect would be insignificant. As will be shown, increases in field intensity and gradient provide an easy means of increasing retention.

EXPERIMENTAL

A block diagram of the magnetic field flow fractionation equipment used in these experiments is shown in Fig. 3. The electromagnet was constructed in our laboratory with a core of cold rolled steel wrapped by 600 m of 18 gauge copper magnet wire. A Lambda (Melville, New York) model LE101M constant current power supply was used to provide dc current from zero to

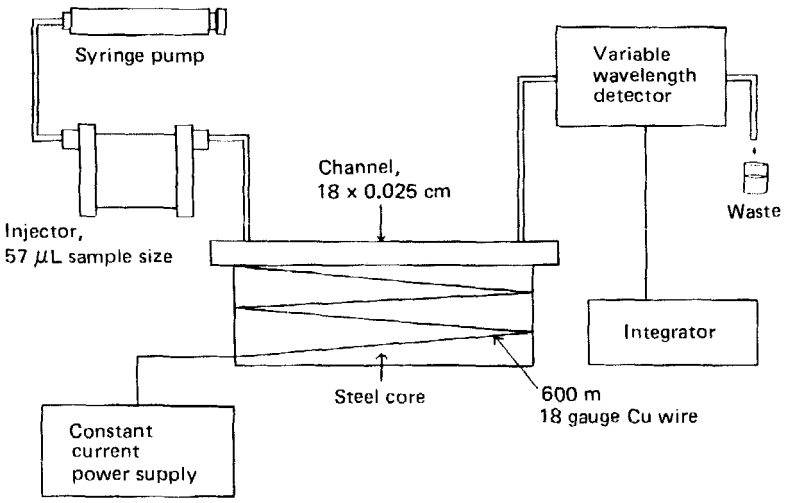

FIG. 3. Block diagram of magnetic FFF experimental equipment.

2.5 A. *Measurements of the magnetic field* were made using a Bell model 640 (Columbus, Ohio) gaussmeter.

Solvent was delivered to the channel from a Sage Instruments (Cambridge, Massachusetts) model 341A syringe pump at flow rates ranging from 50 to 200 μL/min. The channel was formed by clamping a 250-μm thick Mylar spacer between an upper 1/2 in. (1.27 cm) thick glass plate and a lower 1/8 in. (0.32 cm) thick glass plate placed directly on top of the electromagnet core. A special injection valve for introducing the metal oxide particles into the flowing stream was designed and built in this laboratory. This valve was constructed from Teflon and polypropylene with no metal fittings which might tend to attract the magnetic particles. Sample sizes ranging from 10 to 250 μL were available with different rotor positions, with 57 μL being the most commonly used.

The particles were detected by a combination of light scattering and light absorption at 450 nm by using a conventional variable wavelength liquid chromatography detector manufactured by Schoeffel (Westwood, New Jersey) (model 770). Slight modifications were made to the 8 μL flow cell to replace all of the stainless steel tubing and fittings with polypropylene and Kel-F. The detector signal was recorded with a Spectra-Physics (Santa Clara, California) model 4200 computing integrator. The channel void volume value (450 μL) used for retention ratio calculations was measured using the peak maximum retention volume of a sample injected with the

magnet current off. An extra-channel volume of 300 μL was subtracted from the retention volume values prior to calculations.

The iron oxide (Fe_2O_3) particles used were manufactured by Hercules (Wilmington, Delaware) for use in magnetic recording media and were highly monodisperse. These are 0.8 μm long rod-shaped particles with an aspect ratio of 6:1 and a density of 5.2 g/cm^3. Samples were prepared at a concentration of 40 ppm wt/vol in freshly distilled technical grade acetonitrile by ultrasonic mixing and used as a suspension.

RESULTS AND DISCUSSION

Magnetic Field Characterization

Interpretation and prediction of the retention behavior in a FFF system requires an understanding of the applied field. Magnetic FFF requires a field which is uniform along the channel length and as intense as possible, while still having a high field gradient with height in the channel. For our prototype system in order to generate a magnetic field of sufficient intensity which was easily variable, we made use of the basic principles of physics which describe a solenoid (*14*). When current is passed through a wire, a uniform circular magnetic field is generated around the wire. If the wire is formed into a series of loops to produce a coil, the magnetic field of each wire is summed to produce a more intense field. The magnetic field internal to the coil can be further enhanced if a core composed of ferromagnetic material, e.g., iron, is used.

The field internal to a solenoid is quite intense and the field lines are parallel. At the ends of the solenoid the lines diverge and bend around the outside of the coil to complete a continuous path to the opposite pole. The shape of the magnetic field lines along the length of one end of our rectangularly shaped solenoid electromagnet are shown diagrammatically in Fig. 4. The divergence of field lines causes a rapid decrease in field intensity with distance. The equation which describes the magnetic field intensity near the end of a circular solenoid of N turns per meter and area A is

$$B = NAIk(r_1^{-2} - r_2^{-2}) \tag{6}$$

where I is the current, r_1 and r_2 are the distances from the top and bottom of the coil, respectively, and k is the permeability of the core material. This equation is not entirely accurate for the rectangularly shaped coil of our electromagnet. It can be used profitably, however, to understand the shape of

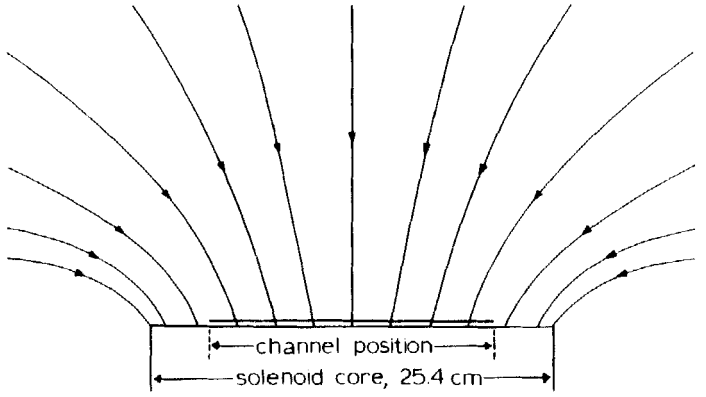

FIG. 4. Magnetic field lines in the vicinity of the FFF channel.

the field and the variation of field intensity with applied current. Figure 5 shows the magnetic field, measured with a gaussmeter, above the solenoid core as a function of distance along the core. The field is very uniform along the length of the FFF channel for all current settings, with less than 10% variation even at the highest current setting of $I = 2.5$ A. A parabolic field shape is obtained at the ends of the solenoid where the coils form a semicircular shape. This is as would be expected from the summation of the field from each individual wire of the coil. It is observed that the field at any point varies directly with applied current, exactly as predicted by Eq. (6). The variation in magnetic field intensity across the top of the solenoid occupied by the channel was measured to be less than 1%. In addition, the residual field produced by magnetization of the iron core was only 3 G after several hundred hours of operation, a value insignificant to our experiment.

The measured variation in the magnetic field intensity with height above the solenoid core is shown in Fig. 6. The inverse square decrease in field intensity with increasing distance predicted by Eq. (6) fits very nearly the field shape as measured with a gaussmeter. Thus, placing the channel as closely as possible to the top of the solenoid provides the most intense field, while also providing the highest available field gradient for an electromagnet of this configuration.

Particle Retention Characterization

In order to determine the amount of agreement between the theoretical description of the magnetic FFF system and actual experimental data, a

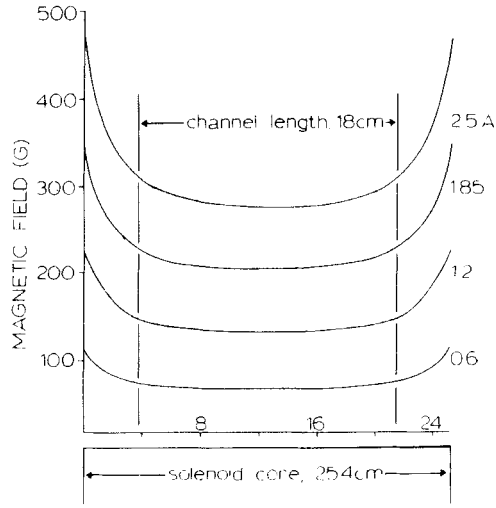

FIG. 5. Magnetic field intensity variation with distance along the solenoid core at four different magnet current settings.

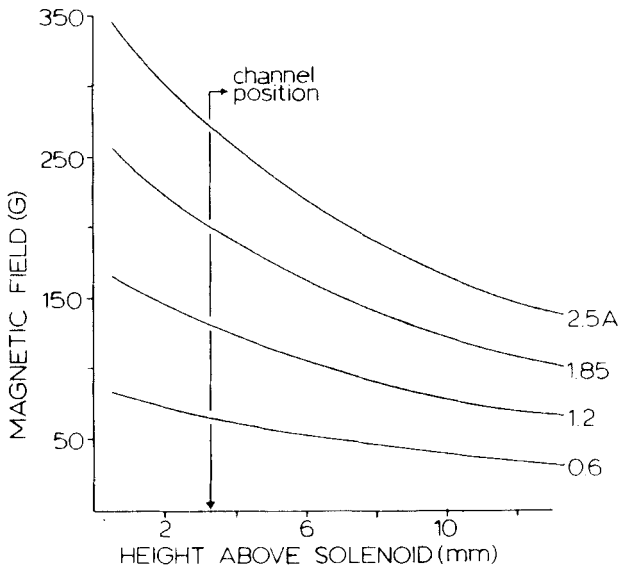

FIG. 6. Variation of the magnetic field intensity with height above the solenoid core at four different magnet current settings. The location of the FFF channel is indicated.

suspension of 40 ppm of iron oxide particles (0.8 μm in length) in acetonitrile with water added as a surface modifier was used as a test sample (*15*). A typical fractogram of this sample is shown in Fig. 7. As predicted by Eqs. (2) and (3), the retention of particles in a FFF system is found to be a function of the force applied to the particles by the external field. The elution volume of the retained fractions of the iron oxide particle suspension is shown in Fig. 8 as a function of the applied magnet current. When interpreted in terms of the fundamental retention equation of FFF, Eq. (2), the dimensionless retention parameter λ can be plotted versus magnet current, Fig. 9. Normally a FFF separation will show a hyperbolic plot of this type; however, magnetic FFF shows a second-order dependence on the field, i.e., magnet current. The reason for this is explained by the form of the magnetic force equation and the solenoid field equation. The field-induced force is a function of the magnitudes of both the field (H) and the gradient (dH/dx), both of which vary with magnet current for a solenoid.

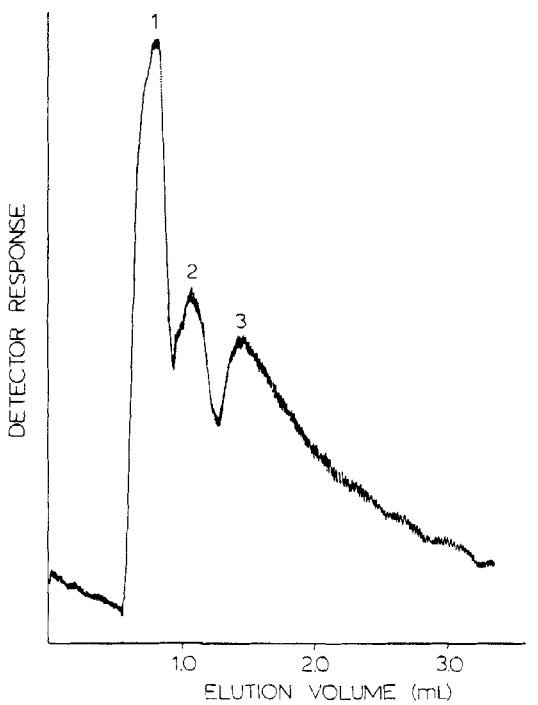

FIG. 7. Fractogram of 0.8 μm iron oxide (Fe_2O_3) particles at a magnet current setting of 1.2 A. Peak 1 is unretained particles, retained Peaks 2 and 3 are single particles and dimers, respectively. A 57-μL sample of a 40-ppm suspension of iron oxide particles in CH_3CN with 5 ppt H_2O was injected in a carrier solvent of CH_3CN (flow rate 100 μL/min).

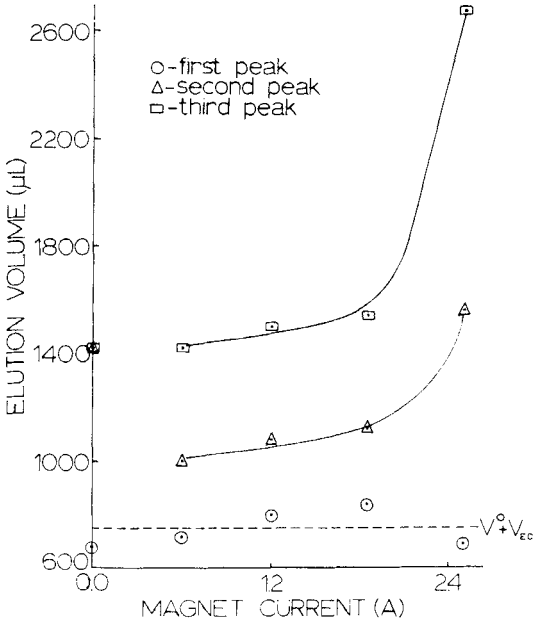

FIG. 8. Elution volume of iron oxide particle fractogram peaks as a function of magnet current. Sample and carrier solvent conditions are the same as shown in Fig. 7.

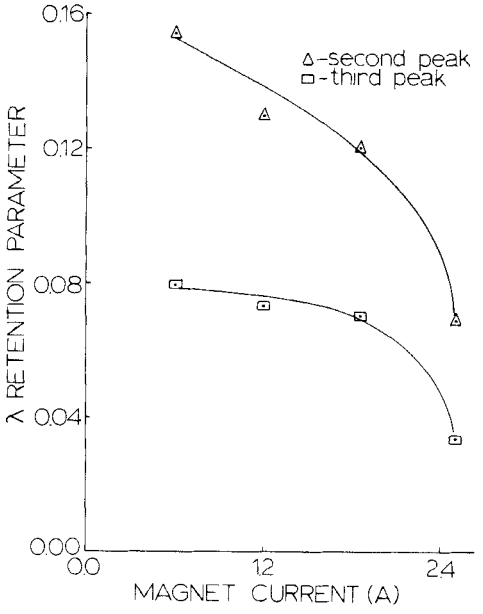

FIG. 9. Retention parameter λ versus magnet current for retained peaks shown in Fig. 8.

The experimental data for iron oxide particles can be replotted as effective magnetic force versus magnet current by using Eq. (3). This provides two curves of similar shape for the peaks observed to elute after the system void volume, Fig. 10. These curves can be compared with that shown in Fig. 11, produced by using Eq. (5) and the measured field intensities. It is seen that the experimental data follow the theoretical curve shape only at high magnet currents. This is reasonable in that over the short channel length of the magnetic FFF (18 cm), true field flow behavior occurs only when a significant percentage of the particles are able to migrate to the lower channel region. A relaxation period was not used in these experiments, as has been done with other FFF techniques, because the very slow sedimentation rate of the particle suspension produced excessive band broadening. The presence of unretained material proved to be advantageous in this work; however, for actual separations applications it will be necessary to work with samples which can settle in a reasonable period of time. The destabilization of metal oxide particle suspensions by means of surfactants is discussed in another paper (*15*).

While the uncertainty in the estimation of the magnetic permeability of the sample and solvent (*13*) as well as the inherent magnetic field of the particles does not allow a direct calculation of the magnitude of the forces from Eq. (5), the ratios of the forces calculated from experimental data provide useful information. The ratio of the experimentally determined forces for Peaks 2

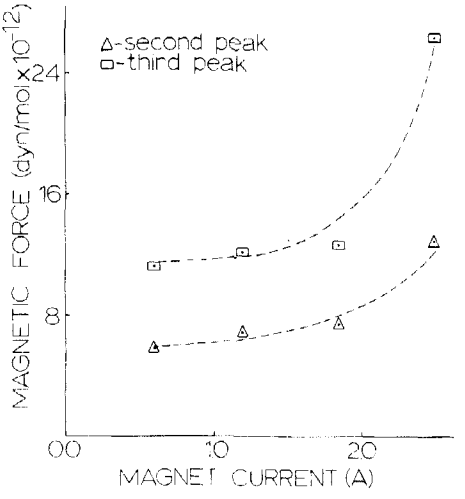

FIG. 10. Experimental magnetic force affecting retained particles as a function of magnet current calculated from the data of Fig. 8 using Eqs. (2) and (3).

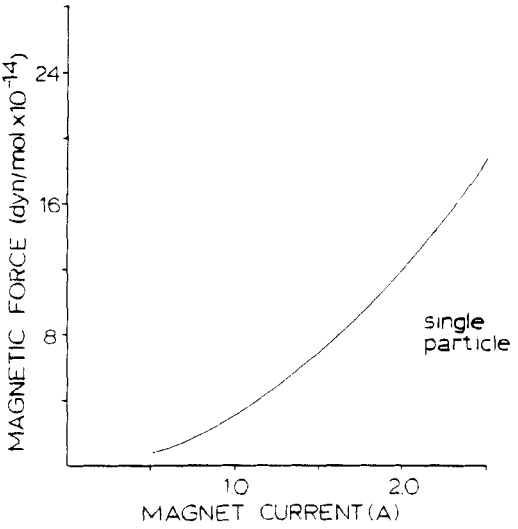

FIG. 11. Theoretical magnetic force affecting retained 0.8 μm iron oxide particles as a function of magnet current. This curve was calculated using Eq. (5), the measured field intensities shown in Figs. 5 and 6, and $\mu_{Fe_2O_3} = 142.7 \times 10^{-6}$, $\mu_{CH_3CN} = -1.1 \times 10^{-6}$.

and 3 are shown in Table 1 as a function of magnet current. These ratios provide a relationship for peak identification when a single type of particle material is present. A ratio of forces predicted by Eq. (5) causes all terms to cancel except for particle volume. It is observed that the force ratio approaches 2.0 as the field strength is increased (Table 1). This indicates that the peaks represent single particles and dimers. The force ratio for lower magnet currents varies to smaller values because of the slow sedimentation of particles into the FFF region. This causes the particles to be less retained than the ideal case. It would be expected that agglomerates containing more than two particles would have progressively larger retention volumes.

TABLE 1
Experimental Magnetic Force Ratio

Magnet current (A)	Force ratio F (Peak 3)/F (Peak 2)
0.6	1.93
1.2	1.77
1.85	1.71
2.5	2.04

However, the probability of larger aggregates being present is low, based upon the kinetics of their formation.

CONCLUSIONS

The experimental and theoretical bases for magnetic FFF have been demonstrated. This addition to the FFF techniques shows great potential for the separation and characterization of solid particles of high magnetic permeability. The model proposed allows the prediction of the magnitude of field strength and/or field gradient necessary to optimize metal oxide particle separations and to extend this technique to other materials.

REFERENCES

1. J. C. Giddings, *J. Chromatogr., 125*, 3 (1976).
2. J. C. Giddings, S. R. Fisher, and M. N. Myers, *Am. Lab.*, p. 15 (May 1978).
3. J. C. Giddings, M. N. Myers, F. J. F. Yang, and L. K. Smith, *Colloid and Interface Science*, Vol. IV (M. Kerker, ed.), Academic, New York, 1976.
4. J. C. Giddings and M. N. Myers, *Sep. Sci. Technol., 13*, 637 (1978).
5. J. C. Giddings, F. J. F. Yang, and M. N. Myers, *Anal. Chem., 46*, 1917 (1974).
6. G. E. Thompson, M. N. Myers, and J. C. Giddings, *Ibid., 41*, 1219 (1969).
7. K. D. Caldwell, L. F. Kesner, M. N. Myers, and J. C. Giddings, *Science, 176*, 296 (1972).
8. J. C. Giddings, F. J. Yang, and M. N. Myers, *Ibid., 193*, 1244 (1976).
9. B. L. Hirschbein, D. W. Brown, and G. M. Whitesides, *Chemtech*, p. 172 (March 1982).
10. L. K. Smith, M. N. Myers, and J. C. Giddings, *Anal. Chem., 49*, 1750 (1977).
11. *Dynamics of Chromatography*, Vol I, Pt. I (J. C. Giddings, ed.), Dekker, New York, 1965.
12. J. C. Giddings, Y. H. Yoon, K. D. Caldwell, M. N. Myers, and M. E. Hoving, *Sep. Sci., 10*, 447 (1975).
13. L. F. Bates, *Modern Magnetism*, Cambridge University Press, London, 1961.
14. P. A. Tipler, *Physics*, Worth, New York, 1976.
15. J. Gorse, T. C. Schunk, and M. F. Burke, *Sep. Sci. Technol.*, Submitted.